Comparative Medicine
Copyright 2010
by the American Association for Laboratory Animal Science

Vol 60, No 5
October 2010
Pages 389–395

Thoracic Radiography as a Refinement Methodology for the Study of H1N1 Influenza in Cynomologus Macaques (*Macaca fascicularis*)

Douglas L Brining,[1,*] John S Mattoon,[3] Lisa Kercher,[1] Rachael A LaCasse,[1] David Safronetz,[2] Heinz Feldmann,[2] and Michael J Parnell[1]

Recent advances in the technology associated with digital radiography have created new opportunities for biomedical research applications. Here we evaluated the use of thoracic radiography as a noninvasive refinement methodology for the cynomologus macaque (*Macaca fascicularis*) model of H1N1 infection. Thoracic radiographic evaluations of macaques infected with any of 3 strains of emerging H1N1 swine-associated influenza virus isolated during the recent pandemic were compared with those of macaques infected with the currently circulating Kawasaki strain of H1N1 influenza. Ventrodorsal, right, and left lateral thoracic radiographs were obtained at days 0, 1, 6, 8, 11, and 14 after infection. A board-certified veterinary radiologist who was blinded to the study design evaluated the images. Numeric scores of extent and severity of lung involvement assigned to each radiograph were compared and demonstrated a significant and substantial difference among groups. The radiographic evaluation allowed for noninvasive assessment of lung involvement, disease onset, progression, and resolution of radiographic changes associated with H1N1 influenza infection.

Abbreviations: KAW, A/Kawasaki/UTK4/2009 influenza strain; CA04, A/California/4/2009 influenza isolate; MEX4108, A/Mexico/4108/2009 influenza isolate; MEX4487, A/Mexico/InDRE4487/2009 influenza isolate.

Swine-origin influenza A (H1N1) was first reported as a newly emerging virus in Mexico in April 2009.[7]The virus rapidly spread worldwide and in June 2009 was categorized as pandemic (level 6) by the World Health Organization.[21,22] The clinical manifestations of the disease in humans include fever, sore throat, vomiting, diarrhea, cough, chills, pneumonia, acute respiratory distress syndrome, and, in some cases, death.[6,7] During the recent pandemic, we acquired 3 newly emerging isolates of swine-origin H1N1 influenza virus: A/Mexico/InDRE4487/2009 (MEX4487), A/California/4/2009 (CA04), and A/Mexico/4108/2009 (MEX4108). MEX4487 was isolated by bronchial aspiration of a 26-y-old man from a family cluster of 3 confirmed severe cases in Mexico. [12] MEX4108 was isolated from a 4-y-old mildly ill boy from Vera Cruz, Mexico, and CA04 was a clinical isolate from a 10-y-old moderately ill boy from California.[8] Both MEX4108 and CA04 were obtained from the United States' Centers for Disease Control and Prevention, Influenza Branch. Our hypothesis was that the newly emerging swine-origin influenza virus isolates would result in more severe clinical symptoms than would the circulating influenza A virus A/Kawasaki/UTK4/2009 (KAW) and that differences in disease severity would be evident by thoracic radiographic evaluation. We were interested in evaluating the efficacy of a numeric radiographic scoring system as a tool for characterizing the differences between groups of cynomologus macaques infected with different influenza isolates and in demonstrating that, because of current digital technology, thoracic radiographic evaluation is practical and should be considered for studies involving respiratory disease as a component of the animal model.

Thoracic radiography is commonly used as a noninvasive diagnostic modality in human and veterinary clinical medicine. The technique is used to evaluate both cardiac and noncardiac thoracic structures.[14,20] During the recent pandemic influenza outbreak, diagnostic radiology reportedly was used for 30% of all patients with known or presumed influenza (H1N1) infection and that the 6% of patients that required ICU stays received an average of 33.5 thoracic radiographic studies during the course of treatment.[18] Characteristic imaging findings in human patients infected with swine-origin influenza A (H1N1) include 'ground glass' opacities, consolidation, and nodular opacities with frequent bilateral lung involvement.[4]

Efforts to refine rodent and nonrodent animal models of infectious diseases and maximize information relative to human clinical disease are an important component of investigating the pathogenesis of viral infection and developing clinical interventions. Newly emerging swine-origin H1N1 influenza virus isolates induce pneumonia and pathologic changes characteristic of its viral etiology as part of the clinical disease process.[11] The purpose of the current study is to determine whether thoracic radiography can be used objectively to determine radiographic differences between groups of cynomologus macaques infected with different strains of newly emerging H1N1 influenza virus

Received: 26 Apr 2010. Revision requested: 29 May 2010. Accepted: 22 Jul 2010.
[1]Rocky Mountain Veterinary Branch and [2]Laboratory of Virology, Rocky Mountain Laboratories, Division of Intramural Research, National Institute of Allergy and Infectious Diseases, National Institutes of Health, Hamilton, Montana; and [3]Department of Veterinary Clinical Sciences, Washington State University, Pullman, Washington.
[*]Corresponding author. Email: briningd@niaid.nih.gov

	Clinical evaluation	Score
Skin and fur	Normal	0
	Ruffled fur, unkempt appearance	5
	Rash, pallor, redness, icterus, petechiae, ecchymoses, wound, abscess, ulcer	10
Nose, mouth, eyes, and head	Normal	0
	Nasal discharge, excessive salivation, ocular discharge, lacrimation, reddened eyes, ptosis	5
Respiration	Normal	0
	Increased or decreased respirations, cough, sneezing	5
	Dyspnea, open mouth breathing, cyanosis	15
Feces and urine	Normal consistency and volume	0
	Decreased feces, dry, wet and pasty, watery feces, discoloration, decreased urine, discoloration	2
	Feces absent	5
	Liquid feces (if debilitating), urine absent, blood in feces or urine	10
Food intake	Normal (eating more than half of the biscuits)	0
	Decreased (eating less than half of the biscuits)	3
	Eating fruit but no biscuits	5
	Severely decreased (not eating biscuits or fruit)	10
Locomotor	Normal	0
	Hyperactivity (circling, increased aggression), hypoactivity (hunched, inactive on camera, active with people in room)	5
	Ataxia, neurologic signs (tremors, head tilt), loss of interest in treats	10
	Reluctant to move, uses cage for support, difficulty getting to food or water (decreased response to human presence), seizures	15
	Down with no or minimal response to human approach, coma	35

Figure 1. Clinical scoring system used to determine humane endpoints in potentially lethal infectious disease models of nonhuman primates. A total clinical score of 35 indicates the need to relieve pain or distress through clinical intervention or euthanasia.

and to demonstrate the value of this noninvasive clinical tool as a methodology for evaluation of disease severity, progression, and resolution.

Materials and Methods

Animals. All subjects were healthy adult (13 male, 14 female) cynomolgus macaques (*Macaca fascicularis*) ranging from 4 to 15 y of age (average, 6.9 y) and weighing between 2.1 and 8.7 kg (average, 4.7 kg). The animals were housed according to regulations and recommendations detailed in the Animal Welfare Act, Public Health Service and NIH Animal Care and Use policies, and the *Guide for the Care and Use of Laboratory Animals*.[3,10,13] The macaques were housed individually in standard nonhuman primate caging (Primate Products, Immokalee, FL) and fed a commercial nonhuman primate diet (Purina 4047, High-Protein Jumbo Biscuits, PMI Nutrition International, St Louis, MO) twice daily. The diet was supplemented with fruit at each feeding. The room was maintained on a 12:12-h light:dark cycle with lights on at 0600. This study was performed at an AAALAC -accredited institution with IACUC approval. Prior to the beginning of the study, all macaques were classified healthy according to physical exam and evaluation of complete blood count, serum chemistry, negative influenza serology, and baseline thoracic radiography.

Infection. The animals were inoculated with either a currently circulating influenza virus A (KAW; $n = 6$) or 1 of 3 newly emerging swine-origin isolates (MEX448, $n = 6$; CA04 $n = 6$; and MEX4108, $n = 9$) from the recent H1N1 pandemic. All isolates were grown on MDCK cells, harvested at a cytopathogenic effect of 3+ (greater than 70% cells were rounded off and detached) for virus stock preparation, and titrated by using a $TCID_{50}$ assay on MDCK cells. The macaques were inoculated under anesthesia (10 mg/kg ketamine IM) with 7×10^6 $TCID_{50}$ through a combination of intratracheal (total volume, 4 mL), oral (total volume, 1 mL), intranasal (0.5 mL per nostril), and intraocular (0.5 mL per eye) inoculation. The oral, intranasal, and intraocular inoculations were done with the animal in dorsal recumbency. A feeding tube (2.7 mm × 41 cm, Argyle, Coviden, Mansfield, MA) was used for intratracheal inoculation. Once the tube was placed with the macaque in dorsal recumbency, the animal was raised into an upright (sitting) position before delivery of the inoculum. All work with the swine-origin isolates was performed under enhanced ABLS3 conditions (Rocky Mountain Laboratories, Division of Intramural Research, National Institute for Allergy and Infectious Diseases, NIH).

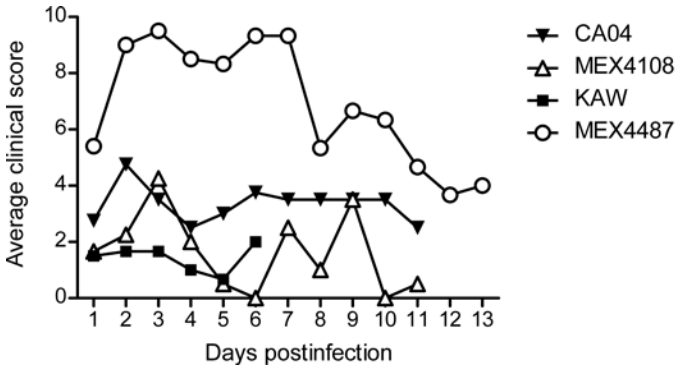

Figure 2. Average clinical score of cynomologus macaques infected with circulating A/Kawasaki/UTK4/2009 (KAW) or swine-origin Mexico/4108/2009 (MEX4108), A/Mexico/InDRE4487/2009 (MEX4487), or A/California/4/2009 (CA04) H1N1 isolates.

Radiography. A mobile digital radiography unit with a flat-panel digital detector (Sound Technologies tru/Dr, Sound-Eklin Carlsbad, CA) was used for obtaining thoracic radiographs. The unit is equipped with a portable X-ray generator (model PXP-HF, Poskom, Korea). The system operates on a veterinary-specific software system (Vetpacs Sound-Eklin). The platform for acquiring images is a modified standard cart (Rubbermaid, Fairlawn, OH). Modifications included a pair of locking wheels that can swivel. The surface of the cart is covered by a custom molded acrylic top that allows for both disinfection of the work surface and protection of the flat-panel digital detector. The macaques were positioned for ventrodorsal radiography by using a polycarbonate V-shaped thoracic positioner. Thoracic radiographs were acquired from ketamine-anesthetized macaques on days 0, 1, 3, 6, 8, 11, and 14 after infection. Radiographic views acquired included ventrodorsal, right lateral, and left lateral thoracic images at peak inspiration. The work surface was surface decontaminated (Clidox, Pharmacal, Naugatuck, CT) after each use. The digital images were interpreted and assigned a numeric score (0 to 3, according to increasing severity) by a veterinary radiologist certified by the American College of Veterinary Radiology who was blinded to the study design. A score was assigned to each set of radiographs (ventrodorsal, right lateral, and left lateral) at each time point. Radiographs were evaluated and scored according to the following criteria: 0, normal examination; 1, mild interstitial pulmonary infiltrates; 2, moderate interstitial infiltrates, perhaps with partial cardiac border effacement and small areas of pulmonary consolidation (alveolar patterns and air bronchograms); and 3, pulmonary consolidation as the primary lung pathology, seen as a progression from grade 2 lung pathology.

Clinical assessment. The health status of the macaques was evaluated through daily visual assessment and physical examinations. A numeric scoring system was used to assign a daily clinical score to each animal. The scoring system included numeric values for the following parameters: posture (0 to 5), respiration (0 to 10), feces and urine production (0 to 10), recumbency (0 to 35), attitude (0 to 5), and evaluation of skin and fur coat (0 to 10; Figure 1). Complete physical exams were performed each time the animals were anesthetized for radiographic evaluation. A numeric score of 35 or greater was predetermined to serve as an endpoint criterion and justification for euthanasia.

Statistical evaluation. The average radiographic score for each group of animals was determined by using JMP software (version 7, SAS, Cary, NC), and the statistical significance of any difference was calculated by using the exact Kruskal–Wallis test, followed by pairwise comparisons to the control group infected with a currently circulating seasonal influenza virus (KAW) by using the Wilcoxon rank sum test (StatXact version 7, Cytel Studio, Cambridge, MA). A one-sided α level of 0.05 was used to determine significance.

Results

The clinical presentation of macaques infected during the study ranged from undetectable disease to moderate disease, according to the clinical scoring system (Figure 2). Common clinical findings included increased body temperature, decreased food and water consumption with corresponding decreases in urine and feces production, and increasing respiratory rates of varying severity. The KAW-infected animals showed mild decreases in food consumption but displayed no additional clinical symptoms. The remaining 3 groups demonstrated varying degrees of anorexia and increases in respiratory rate, with the group infected with MEX4478 having the highest overall averages for clinical score. Complete blood chemistry and clinical analysis were performed at each radiographic evaluation for all groups and were characterized by an initial mild to moderate transient lymphopenia and unremarkable clinical chemistry parameters (data not shown). No macaques in the study groups had a clinical presentation that necessitated euthanasia, although animals were euthanized at predetermined time points as part of a larger pathogenesis evaluation.

The severity of radiographic lesions associated with infection ranged from very mild in KAW-infected macaques to severe in those infected with MEX4108, MEX4487, and CA04. Right lateral and ventrodorsal baseline radiographs obtained before infection were compared with corresponding radiographs at day 6 after infection with the respective influenza isolates (Figure 3). The veterinary radiologist determined that all baseline radiographs were normal examinations (grade 0), with no radiographic changes associated with respiratory infection. On day 6 after infection, the radiographic interpretation for KAW-infected animals also was evaluated as normal, indicating no radiographically apparent disease. The MEX4108 isolate was characterized at day 6 after infection as causing grade 3 changes with right middle lung lobe interstitial infiltrate and consolidation, which included ventral aspects of the lung field and right cardiac border effacement. MEX4487 day 6 after infection radiographs were scored as having grade 3 changes described as bilateral middle and caudal lung lobe consolidation. CA04 day 6 postinfection was scored as grade 3 changes described as severe progressive pneumonia with right middle, right cranial, and caudal lung consolidation with a middorsal distribution. Macaques infected with MEX4108 and MEX4487 demonstrated peak radiographic changes at day 6. For macaques infected with CA04, the severity of these lesions continued to progress and peaked by day 8 after infection. We found that interstitial infiltration was present in 16% (1 of 6) of the KAW-infected macaques, 67% (4 of 6) in each group of CA01- and MEX 4108-infected animals, and 89% (8 of 9) of the MEX4487-infected macaques.

The radiographs allowed for evaluation of onset, progression, and resolution of radiographic lesions associated with each of

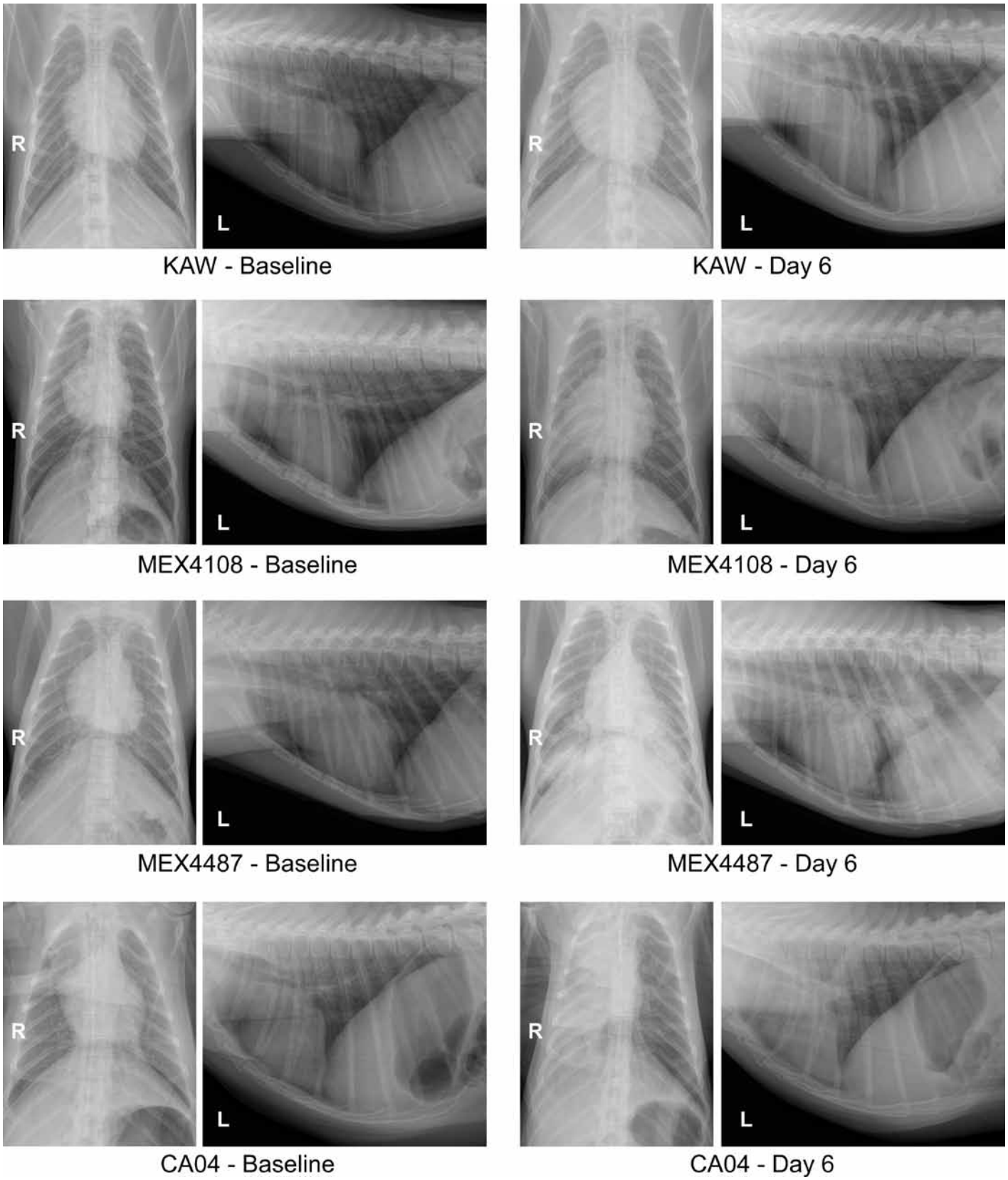

Figure 3. Ventrodorsal and left lateral thoracic images of cynomologus macaques at baseline and day 6 after infection with circulating A/Kawasaki/UTK4/2009 (KAW) or swine-origin Mexico/4108/2009 (MEX4108), A/Mexico/InDRE4487/2009 (MEX4487), or A/California/4/2009 (CA04) H1N1 isolates.

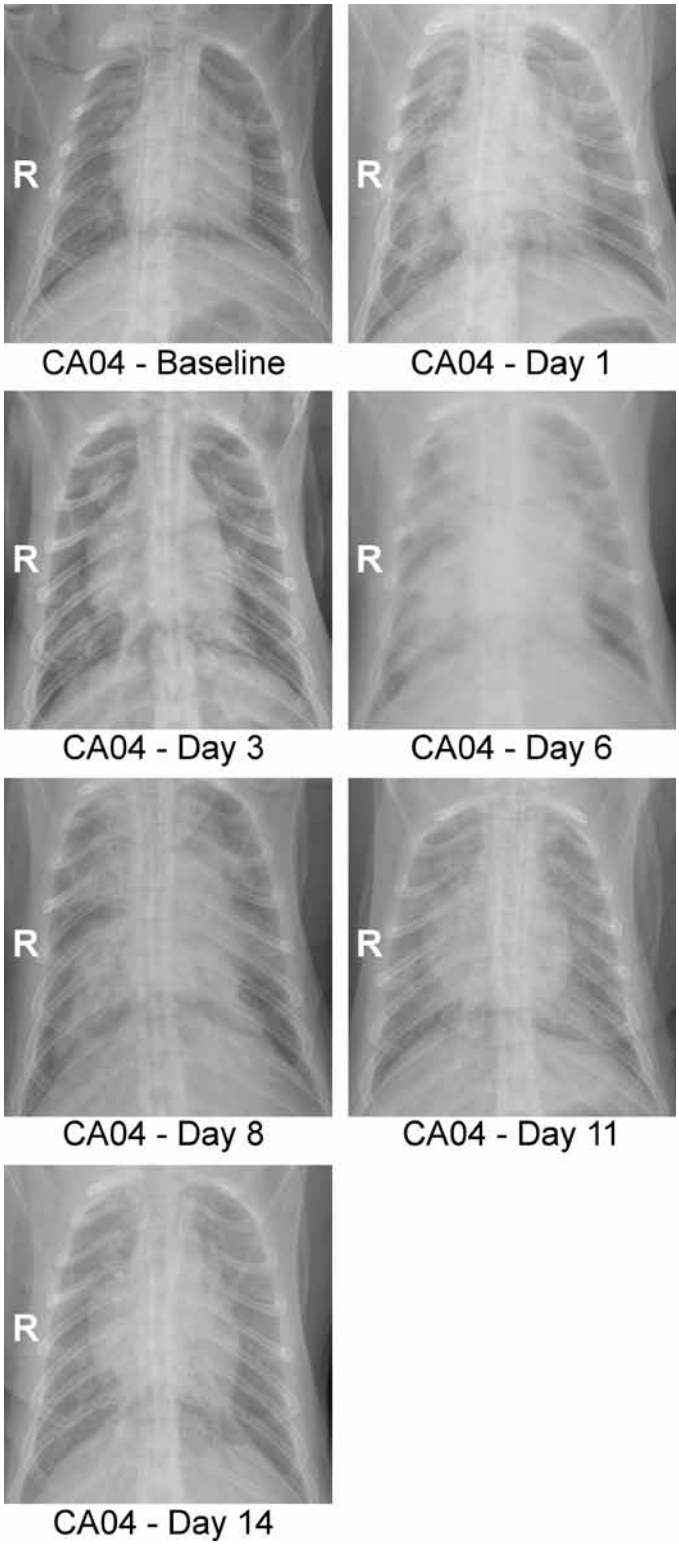

Figure 4. Ventrodorsal thoracic radiographs (baseline through day 14 after infection) of a cynomologus macaque infected with A/California/4/2009. Radiographically the infection was characterized by progressive interstitial and alveolar infiltrate with peak severity on day 6 and day 8 and followed by resolution of radiographic changes.

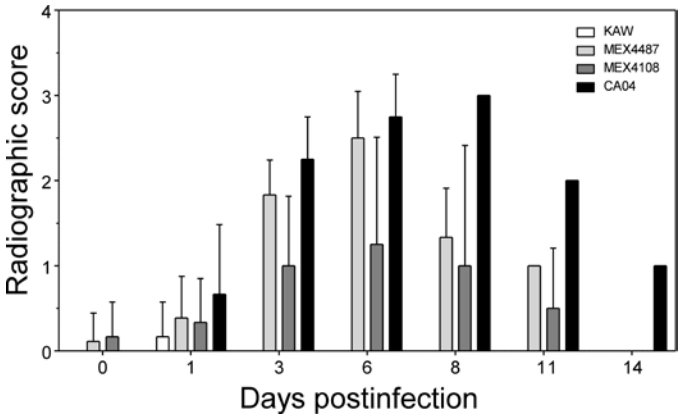

Figure 5. Radiographic score (mean ± SE) for groups of animals infected with A/Kawasaki/UTK4/2009 (KAW) or the swine-origin Mexico/4108/2009 (MEX4108), A/Mexico/InDRE4487/2009 (MEX4487), or A/California/4/2009 (CA04) H1N1 isolates. Grade 0, normal examination; grade 1, mild interstitial pulmonary infiltrates; grade 2, moderate interstitial infiltrates perhaps with partial cardiac border effacement and small areas of pulmonary consolidation (alveolar patterns and air bronchograms); and grade 3, pulmonary consolidation as the primary lung pathology, seen as a progression from grade 2 lung pathology.

the 4 influenza isolates. Figure 4 shows ventrodorsal radiographs from a representative macaque infected with CA04, over the time course of the study. The baseline radiograph was scored as grade 0. On day 1, the right cranial, middle, and caudal lung lobes showed interstitial and alveolar infiltrate primarily in the perihilar region. By day 3 after viral exposure, there is evidence of moderate progressive left middle and caudal lung infiltrates, primarily perihilar but with mild ventral consolidation. Radiographs taken on days 6 and 8 after infection show progressive right and left lung consolidation with complete cardiac border effacement. Multiple air bronchograms are present both bilaterally and ventrally. Day 11 of infection is characterized by partial resolution of consolidation; however, interstitial infiltrates remain evident bilaterally. By day 14 after infection, there was continued resolution to changes described as diffuse mild interstitial infiltrates.

Average radiographic scores were compared between the KAW-infected group and each of those infected with the swine-origin emerging influenza viruses MEX4487, CA04, or MEX4187 isolates (Figure 5). A numeric score on a scale of 0 to 3 based on severity of radiographic changes was assigned to each set of radiographs (ventrodorsal, right lateral, and left lateral). The circulating KAW virus led to only minor radiographic change on day 1 after infection, and no detectable changes from baseline were noted throughout the remaining time points. Both MEX4487 and MEX4108 yielded similar patterns of radiographic changes, and differences were not statistically significant. Both MEX4487 and MEX4108 caused detectable radiographic changes on day 1 after inoculation, and peak radiographic changes were observed on day 6 postinfection. After the peak scores on day 6, both MEX4487 and MEX4108 were characterized by a decreasing radiographic scores that returned to baseline, indicating resolution of detectable clinical disease by day 14 after inoculation. The CA04 isolate led to the highest average radiographic score at all time points. The onset of radiographic changes occurred on day1, and the peak radiographic score was on day 8 after infection. Thereafter, CA04 showed a trend of decreasing radiographic scores to day

14 after inoculation; the radiographic score had not returned to baseline by day 14.

Statistical evaluation of the average radiographic scores for days 0 through 6 for each monkey was accomplished by the use of an exact Kruskal–Wallis test. The *P* value from this exact test was 0.001, suggesting a significant and substantial difference between the average scores of the groups. Because the working hypothesis was that the pandemic H1N1 viruses would result in more severe disease and subsequent radiographic changes, pairwise comparisons of KAW with MEX4108, MEX4487, and CA04 were performed by using Wilcoxon rank sum tests. The resulting one-sided *P* values of 0.012, 0.029, and 0.029, support the theory that each of the new isolates MEX4108, MEX4487, and CA04 resulted in radiographic changes that were significantly different from those associated with the previously circulating KAW influenza strain.

Discussion

The clinical presentation of the infected macaques was consistent with the radiographic findings. Although the average clinical scores of the 4 groups did not differ significantly, they were consistent with the assigned radiographic scores. The KAW-infected animals showed minimal evidence of clinical disease and had the lowest average radiographic score of the 4 groups. The MEX4108-infected group was characterized by relatively mild clinical symptoms and demonstrated higher average radiographic scores than did the KAW-infected group. Macaques infected with CA04 and MEX4487 demonstrated the highest average radiographic and clinical scores. In general, we noted that across all groups, a pattern of decreasing clinical score corresponded with resolution of radiographic changes.

The radiographic findings from the cynomolgus macaque model were consistent with those reported from radiographic and computer tomographic studies of humans infected with swine-origin influenza virus. The most commonly reported imaging finding among humans was unilateral or bilateral ground-glass opacities with or without associated focal or multifocal consolidation.[1,2,4] In the cited studies, ground-glass opacity was defined as hazy areas of increased opacity without obstruction of underlying vessels or structures. This definition correlates with what we describe as interstitial infiltration or opacity in the current study. This interstitial infiltration often progressed to areas of consolidation in macaques infected with the strains of newly emerging influenza virus. In addition, air bronchograms could be detected in one-third of human patients in another study,[4] and midlung areas were the most frequently affected. These findings also were common in our macaque model of swine-origin H1N1 infection.

The results of the present study demonstrate that time-course thoracic radiographs have scientific value as a noninvasive refinement methodology for evaluation of an emerging respiratory pathogen. Although film-based radiography has been impractical for research applications that required the acquisition of multiple radiographs from large numbers of research subjects, recent advances in the technology associated with digital radiography and the increased availability of the equipment have created new opportunities for biomedical research applications. Refinement of research methodologies is an underlying principle in the use of animals as research subjects in biomedical investigations. Maximizing the amount of valuable information from any given experiment is an essential component of the '3Rs' concept of replacement, reduction, and refinement.[17] In the current radiographic study, we were able to use an additional tool to show the statistically significant differences in radiologic changes associated with active disease of 4 different strains of H1N1 influenza viruses. We were able to characterize the onset of disease as well as peak severity and partial to complete resolution of radiographic changes and to make correlations to clinical presentations.

Many newly emerging pathogens with significant human health implications, including Hendra virus, Nipah virus, SARS coronavirus, and influenza viruses, have the potential for respiratory disease as component as part of the clinical progression.[5,15,19] Animal models are being developed and used to further characterize the pathogenesis, pathophysiology, and potential treatment strategies for these diseases.[9,16] Although more advanced imaging modalities, including MRI and positron-emission tomography–computerized tomography combinations, are being used in various aspects of biomedical research, the increased availability of digital radiographic units makes this option potentially attractive. Thoracic radiologic evaluation is a simple, cost-effective, and often overlooked tool for further characterizing disease processes in animal models.

Acknowledgments

This research was supported by the Division of Intramural Research of National Institute of Allergy and Infectious Diseases, NIH. We thank Barry Rockx, Friederike Feldmann, Don Gardner, Andrea Marzi, Hideki Ebihara, Anthony York, William Shupert, and Dan Long for their scientific contributions to the larger swine-origin H1N1 influenza pathogenesis study. We also thank Edward Schreckendgust, Rocky Rivera, Sandy Skorupa, and Kathleen Meuchel for their assistance with animal care and sample collection. We are thankful to Martha Nason and Anita Mora for their assistance with the statistical evaluation of the radiographic scores and preparation of the radiographic images, respectively.

References

1. **Agarwal PP, Cinti S, Kazerooni EA.** 2009. Chest radiographic and CT findings in novel swine-origin influenza A (H1N1) virus (S-OIV) infection. Am J Roentgenol **193:**1488–1493.
2. **Ajlan AM, Quiney B, Nicolaou S, Muller NL.** 2009. Swine-origin influenza A (H1N1) viral infection: radiographic and CT findings. Am J Roentgenol **193:**1494–1499.
3. **Animal Welfare Act as Amended.** 2007.7 USC §2131-2159.
4. **Aviram G, Bar-Shai A, Sosna J, Rogowski O, Rosen G, Weinstein I, Steinvil A, Zimmerman O.** 2010. H1N1 influenza: initial chest radiographic findings in helping predict patient outcome. Radiology **255:**252–259.
5. **Bodewes R, Rimmelzwaan GF, Osterhaus A.** 2010. Animal models for the preclinical evaluation of candidate influenza vaccines. Expert Rev Vaccines **9:**59–72.
6. **Centers for Disease Control and Prevention.** [Internet]. 2009. Interim guidance for clinicians on identifying and caring for patients with swine-origin influenza (H1N1) virus infection. [Cited 1 Mar 2010]. Available at: www.cdc.gov/h1n1/flu/identifyingpatients.htm.
7. **Centers for Disease Control and Prevention.** 2009. Outbreak of swine-origin influenza A (H1N1) virus infection—Mexico, March–April 2009. Morb Mortal Wkly Rep **58**:467–470.
8. **Centers for Disease Control and Prevention.** 2009. Swine influenza A (H1N1) infection in 2 children—Southern California, March–April 2009. MMWR Morb Mortal Wkly Rep **58:**400–401.
9. **Geisbert TW, Daddario-Dicaprio KM, Hickey AC, Smith MA, Chan YP, Wang LF, Mattapallil JJ, Geisbert JB, Bossart KN, Broder CC.** 2010. Development of an acute and highly pathogenic nonhuman primate model of Nipah virus infection. PLoS One **18:**e10690.

10. **Institute for Laboratory Animal Research.** 1996. Guide for the care and use of laboratory animals. Washington (DC): National Academies Press.
11. **Itoh Y, Shinya K, Kiso M, Watanabe T, Sakoda Y, Hatta M, Muramoto Y, Tamura D, Sakai-Tagawa Y, Noda T, Sakabe S, Imai M, Hatta Y, Watanabe S, Li C, Yamada S, Fujii K, Murakami S, Imai H, Kakugawa S, Ito M, Takano R, Iwatsuki-Horimoto K, Shimojima M, Horimoto T, Goto H, Takahashi K, Makino A, Ishigaki H, Nakayama M, Okamatsu M, Takahashi K, Warshauer D, Shult PA, Saito R, Suzuki H, Furuta Y, Yamashita M, Mitamura K, Nakano K, Nakamura M, Brockman-Schneider R, Mitamura H, Yamazaki M, Sugaya N, Suresh M, Ozawa M, Neumann G, Gern J, Kida H, Ogasawara K, Kawaoka Y.** 2009. In vitro and in vivo characterization of new swine-origin H1N1 influenza viruses. Nature **460:**1021–1102.
12. **Kobinger GP, Meuiner I, Patel A, Gre J, Stebner S, Leung A, Neufeld JL, Kobasa D, von Messling V.** 2010. Assessment of the efficacy of commercially available vaccines against pandemic H1N1 2009 virus. J Infect Dis **201:**1000–1006.
13. **Office of Laboratory Animal Welfare.** [Internet]. 2002. Public health service policy on humane care and use of laboratory animals. [Cited 1 Mar 2010]. Available at: http://grants.nih.gov/grants/olaw/references/phspol.htm.
14. **Owens JM, Biery DN.** 1992. Radiographic interpretation for the small animal clinician, 2nd ed. Baltimore (MD): Williams and Wilkins.
15. **Peiris JS, Guan Y, Yuen KY.** 2004. Severe acute respiratory syndrome. Nat Med **10:**S88–S97.
16. **Rockx B, Bossart K, Feldmann R, Geisbert JB, Hickey AC, Brining D, Callison J, Safronetz D, Marzi A, Kercher L, Long D, Broder CC, Feldmann H, Geisbert TW.** 2010. A novel model of lethal Hendra virus infection in African green monkeys and the effectiveness of ribavirin treatment. J Virol [Epub ahead of print].
17. **Russell WMS, Burch RL**. 1959. The principles of humane experimental technique. Wheathampstaed (UK): Universities Federation for Animal Welfare.
18. **Schafer JR, Agarwal P, Kazerooni E.** 2010. Radiology resource utilization during an H1N1 influenza outbreak. J Am Coll Radiol **7:**28–32.
19. **Selvey LA, Wells RM, McCormick SG, Ansford AJ, Murray K, Rogers RJ, Lavercombe PS, Selleck P, Sheridan JW.** 1995. Infection of human and horses with newly described morbilllivirus. Med J Aust **162:**642–645.
20. **Thrall DE.** 1994. Textbook of veterinary diagnostic radiology, 2nd ed. Philadelphia (PA): WB Saunders.
21. **World Health Organization.** [Internet]. 2009. Global alert and response: current WHO phase of pandemic alert. [Cited 1 Mar 2010]. Available at: www.who.int/csr/disease/avian_influenza/phase/en/index.hmtl.
22. **World Health Organization**. [Internet]. 2009. World now at the start of 2009 influenza pandemic. [Cited 1 Mar 2010]. Available at: www.who.int/mediacenter/news/statements/2009/h1n1_pandemic_phase6